Context-dependent adaptation improves robustness of myoelectric control for upper-limb prostheses

Patel, Gauravkumar K.; Hahne, Janne M.; Castellini, Claudio; Farina, Dario; Dosen, Strahinja

Published in:
Journal of Neural Engineering

DOI (link to publication from Publisher):
10.1088/1741-2552/aa7e82

Publication date:
2017

Document Version
Accepted author manuscript, peer reviewed version

PAPER

Context-dependent adaptation improves robustness of myoelectric control for upper-limb prostheses

To cite this article: Gauravkumar K Patel *et al* 2017 *J. Neural Eng.* **14** 056016

Context-Dependent Adaptation Improves Robustness of Myoelectric Control for Upper-Limb Prostheses

Gauravkumar K. Patel[1], Janne Hahne[1], Claudio Castellini[2], Dario Farina[1,3], Strahinja Dosen[1]

- [1] *Neurorehabilitation Systems Research Group, Department of Trauma Surgery, Orthopedics and Plastic Surgery, University Medical Center Göttingen, 37075 Göttingen, Germany.*
- [2] *Institute of Robotics and Mechatronics, DLR - German Aerospace Center, D-82234 Wessling, Germany*
- [3] *Department of Bioengineering, Imperial College London, London, UK.*

Keywords: *myoelectric control, upper-limb prosthesis, context driven control*

Corresponding Author:
Strahinja Dosen (strahinja.dosen@bccn.uni-goettingen.de)

Abstract:

Objective. Dexterous upper-limb prostheses are available today to restore grasping, but an effective and reliable feed-forward control is still missing. The aim of this work was to improve the robustness and reliability of myoelectric control by using context information from sensors embedded within the prosthesis. *Approach.* We developed a context-driven myoelectric control scheme (cxMYO) that incorporates the inference of context information from proprioception (inertial measurement unit) and exteroception (force and grip aperture) sensors to modulate the outputs of myoelectric control. Further, a realistic evaluation of the cxMYO was performed online in able-bodied subjects using three functional tasks, during which the cxMYO was compared to a purely machine-learning-based myoelectric control (MYO). *Main Results*. The results demonstrated that utilizing context information decreased the number of unwanted commands, improving the performance (success rate and dropped objects) in all three functional tasks. Specifically, the median number of objects dropped per round with cxMYO was zero in all three tasks and a significant increase in the number of successful transfers was seen in two out of three functional tasks. Additionally, the subjects reported better user experience. *Significance.* This is the first online evaluation of a method integrating information from multiple on-board prosthesis sensors to modulate the output of a machine-learning-based myoelectric controller. The proposed scheme is general and presents a simple, non-invasive and cost-effective approach for improving the robustness of myoelectric control.

1 Introduction

Reliability of myoelectric control is a challenge in wearable robotics, particularly in relation to dexterous control of upper-limb prostheses [1]. Our surroundings are organized in such a way that the arms and hands are necessary to complete most routine activities and therefore it is not surprising that the loss of the upper limb, partial or total, represents a severe impairment. With current technological advances, the missing limb can be replaced with a dexterous prosthesis, but an efficient and user-friendly control of these systems is still an open problem. The rejection rates for myoelectric prostheses are about one third for pediatric and one fourth for adult patients [2]. In general, the control strategy interfacing the patient with the prosthesis is the critical bottleneck.

In the last three decades, many classification- and regression-based control algorithms have been proposed for control of dexterous upper-limb prostheses [3]–[6]. While these algorithms show encouraging results in laboratory conditions, the majority of them have not been translated to the clinical market. The main problem is the lack of robustness during daily use, as the performance is sensitive to arm position, electrode repositioning and muscle fatigue [7]. For this reason, most clinically available solutions still use the classic two-channel sequential and proportional control, in which a pair of muscles is used to control a single DoF and coactivation is employed to switch between the DoFs [8]. There is only one, recently presented commercial solution implementing control based on pattern classification [9].

The pattern classification and regression methods used for prosthesis control follow the same paradigm, i.e., the user generates a control signal, which is detected using sensors, and the sensor data are presented to a classifier/regressor to generate prosthesis commands. The required control signal is mostly generated via muscle activations (EMG sensing [5], sonomyography [10], mechanomyography [11], multimodal detection [12]), or occasionally via user motion (inertial units [13], [14]). The usage of additional information, apart from the direct control signal(s), has rarely been considered in the

framework of machine learning for prosthetic control. Even when additional information has been used, the implementation has followed the conventional black-box paradigm, i.e., all available information is presented as an input to the classifier. For example, to mitigate the effect of arm position on prosthesis control, inertial data was given as an input to a multimodal (EMG and inertial data) pattern classifier in [15]. In a two-stage implementation [16], a unimodal position classifier was used to estimate the arm position based on inertial data. This estimate was then used to select a unimodal EMG classifier (trained for that arm position) to identify user intention.

However, context information, including all data describing the state of the system, environment and the user, apart from the direct volitionally generated control signals, has a great potential to facilitate prosthesis control. For example, computer vision and inertial sensors have been integrated within the framework of semi-autonomous prosthesis control to automatically adjust wrist rotation and hand preshaping [17], [18]. In this scheme, a simple two-channel myoelectric interface was used to trigger, correct and fine tune the automatic decisions made by the system (i.e., triggering/correcting the automatic adjustment of wrist or hand preshaping). Sensors embedded into the prosthesis were employed to activate automatic slip prevention [19] or to automatically select grasp type (palmar or lateral) based on contact location [20], i.e., palmar grasp was triggered if the contact was detected on the fingertip and key grip was activated in response to the detection on the lateral aspect of the index finger. In a state-based control scheme, users employed direct control [21] and pattern classification [22] to trigger the state transition(s). In each state, the context information detected by the prosthesis sensors was used to implement a specific function automatically (e.g., prevention of slipping). In all these cases, however, the context sensing was used to automatize prosthesis functions and not to improve the performance of a machine learning controller.

In the present study, we demonstrate a novel approach as to how context information from additional sensors can be used to improve the performance of machine-learning-based myoelectric control. The approach is called *context-driven myoelectric control (cxMYO)*. Specifically, a context-driven myoelectric control is defined as a system that utilizes information gathered from supplementary sensors (e.g. inertial sensors) to modulate the parameters of a conventional machine-learning-based myoelectric controller. The novel method is more general compared to previous approaches [16], [15] and allows inclusion of context information from a variety of sensors embedded within the prosthesis (e.g. force, aperture, inertial units). The novel approach was evaluated online in three functional tasks to test its robustness, and the performance was compared to that of a machine-learning-based myoelectric control. The novel method is presented in Section 2 and the functional tasks are described in Section 3. The results of the online evaluation are reported in Section 4 and Section 5 concludes the work with a summary and general discussion.

2 Methods and Material

2.1 The novel concept

The novel concept is depicted in Fig. 1. The main idea is to exploit information from various on-board prosthesis sensors to improve sequential and proportional control of a dexterous prosthesis. Most commercial and research prostheses are equipped with sensors that provide proprioceptive (joint angles) and/or exteroceptive (grasping force) information. However, this information has not been used to improve prosthesis control based on machine learning. Traditionally, pattern classification and

regression is employed to define an invariant mapping function between the user's muscle activity and the prosthesis commands; the mapping function is determined during a controller training phase. In the novel approach (Fig. 1), we propose to adapt this mapping online based on the state of the prosthesis (context information) detected using embedded proprioceptive and exteroceptive sensors. More specifically, we propose a new control framework called the *context-driven myoelectric control (cxMYO)* comprising of two interacting units: a context-aware component (CAC) and a conventional myoelectric controller (MYO). The CAC infers context information (e.g., the state of the prosthesis) based on real-time sensor data and this information is used to modulate the parameters of the MYO. Therefore, the mapping between the user's muscle activity and the generated prosthesis command (defined by MYO) becomes reactive to the inferred context information. In this study, we present one specific implementation of the general conceptual scheme in Fig. 1. The presented cxMYO implementation contains a CAC unit which only modulates the outputs of the MYO, leaving its internal parameters unchanged. Another implementation of the general scheme in Fig. 1 can include a CAC unit that would use context information to update the internal parameters of the MYO. For example, the class prior probability of each prosthesis command could be modulated depending on the detected prosthesis state.

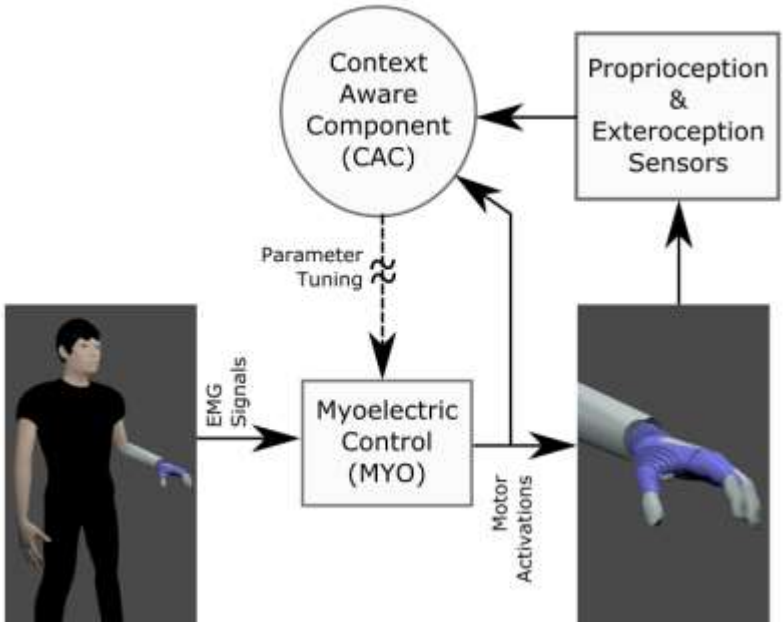

Fig. 1: Conceptual scheme of the proposed context-driven myoelectric control (cxMYO). The scheme integrates a state-of-the-art machine-learning-based myoelectric interface (MYO) and an automatically driven context-aware component (CAC). The context inference is realized by the CAC using proprioceptive (e.g., orientation and position) and exteroceptive (e.g., force) sensors embedded within the prosthesis. Based on the inferred context, the parameters (e.g., activation thresholds) of MYO are adjusted in real-time.

2.2 Implementation

2.2.1 System Components

The prototype system (Fig. 2) used for the present experiment comprised a wireless Myo armband (Thalmic Labs, Canada) and a Michelangelo hand prosthesis (Otto Bock, DE) equipped with a

wrist rotator. The armband was placed approximately 5 cm below the elbow joint of the left forearm. It integrated eight EMG acquisition channels using dry electrodes and an inertial measurement unit (IMU). The armband was oriented so that the positive X-axis of the IMU was parallel to the forearm axis, pointing towards the volar side of the wrist. The IMU provided the 3-D orientation of the subject forearm (yaw, pitch and roll), as if the sensor was embedded into the prosthetic socket. The EMG data was sampled at 200 Hz and transferred at the same rate to the host PC via a Bluetooth interface for further processing. The prosthetic hand was attached to the subject forearm using a custom made splint. The hand was capable of performing two grasp types (palmar and lateral). It was equipped with an embedded force and aperture sensor, each with a resolution of 100 levels – where the maximum sensor value corresponded to the maximum grasping force (~100 N) and hand aperture (~11 cm for palmar and ~7 cm for lateral grasp), respectively. All prosthesis functions (grasping and rotation) were controlled using velocity commands, prescribing the desired velocity of closing/opening and pronation/supination. A Bluetooth interface allowed the host PC to send the normalized control commands to the hand and receive sensor data from the hand, sampled at the rate of 100 Hz. An additional wireless IMU (MTx, Xsens, NE) was placed on the upper arm to determine its orientation. The positive X-axis of the sensor was aligned with the X-axis of the Myo armband, pointing towards the elbow crease. However, this unit was not a part of the control system and it was only used for the assessment of user movement. Therefore, in the future, all components (8 EMG electrodes and forearm inertial unit) required for control can be integrated into a socket, leading to a self-contained solution. A standard Windows 7 desktop computer (Intel i5, 3.3 GHz, 8 GB RAM) was used to implement an online myoelectric control software as a standalone C# program (Microsoft Visual Studio 2015).

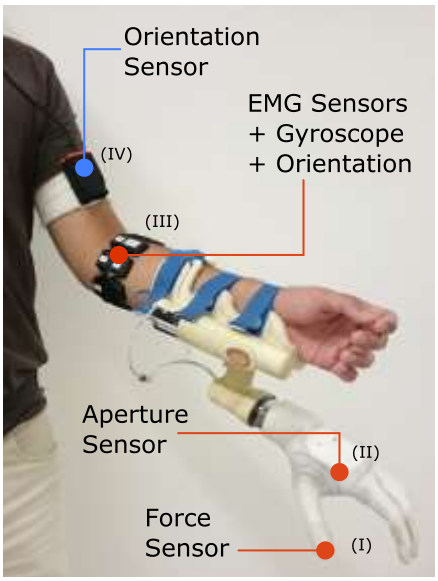

Fig. 2: The hardware setup comprised a Michelangelo hand prosthesis (Otto Bock, Germany) with embedded force (I) and aperture sensor (II), a Myo-bracelet (III, Thalmic Labs, Canada) integrating eight sEMG-channels and an embedded inertial unit with a 3-axes gyroscope and a 3-axes orientation sensor. In addition, (IV) an inertial measurement unit (Xsens, Netherlands) was placed on the upper arm to detect its orientation. Importantly, this sensor (IV) was employed to calibrate the experiment and it was not required for control. All control system components could be embedded into the prosthetic socket, thereby achieving a self-contained solution.

2.2.2 Myoelectric Controller

A modified version of the approach presented in [23] using incremental Ridge Regression with Random Fourier Features (see Appendix) was implemented for the sequential and proportional control

of five prosthesis functions, namely, wrist pronation, wrist supination, palmar grasp closing, lateral grasp closing and hand opening. These prosthesis functions were mapped to five dynamic contraction patterns, namely, to wrist radial and ulnar deviation, wrist flexion, closed fist and wrist extension, respectively, as in [24].

Model Training: The training data for each pattern was collected by comfortably contracting the muscles for five seconds to approximately 60% of the maximum voluntary contraction (MVC). The subjects stood upright with their elbow flexed at 90° while wearing the socket connected to the prosthesis. Additionally, the pattern *rest* that corresponds to no prosthesis motion was trained using both static and dynamic conditions. For the static-rest, the subjects were asked to relax the wrist and hand for 5 s while maintaining the elbow at 90° flexion. For the dynamic-rest, the subjects were asked to move the elbow and shoulder while keeping the wrist and hand relaxed. These patterns were included to reduce commonly observed unwanted movement predictions made by the machine learning model, when spurious EMG activations are observed during dynamic arm movement(s). The following four dynamic-*rest* movements were trained: 1) repetitive elbow flexion/extension between 0° and 90° for five seconds. 2) repetitive medial and lateral rotation of the shoulder (i.e. forearm moving left and right) for five seconds, 3) repetitive shoulder flexion between 0° and 90° for five seconds and 4) repetitive shoulder abduction and adduction for five seconds. As the approach supports incremental learning [23], it was possible to re-evaluate the model by adding more training samples for any particular pattern. Before starting the experiment, this was done to improve the quality of myoelectric prediction and assure the same baseline quality of control across subjects. The quality of control was examined by asking the subjects to produce the command signals for each prosthesis function in four different arm positions, namely, forearm down, elbow flexed, arm frontally extended and arm laterally extended. Specifically, in each arm position, the subject was asked to activate each prosthesis function proportionally between 0 to 80% of the normalized activation. If the subjects had difficulties in activating a particular prosthesis function and/or he could not modulate the activation within the range 0-80%, the prosthesis control was deemed not good enough and the respective pattern was incrementally trained in that position. An on-screen digital oscilloscope embedded within our myocontrol framework was used to visually verify the activation of each prosthesis function.

Online Control: For each acquisition channel, the root-mean-square (RMS) envelope was evaluated every 5 ms using a window size of 150 ms and then, a digital first-order low-pass Butterworth filter with the cutoff frequency of 2 Hz was applied to smooth the envelope. The input for online prediction was the most recent sample of the filtered EMG envelope and the outputs were the estimated values of normalized velocity for the five prosthesis functions. The output was predicted at a rate of 100 Hz and was further low-pass filtered using a first-order Butterworth filter with a cut-off frequency of 3 Hz. Next, a threshold T (default value 0.2) was applied to the estimated velocities to remove the uncertainty at low contraction levels and the obtained values were then multiplied by a fixed gain G (of 1.25 for grip open/close and 1.00 for wrist rotation). Therefore, the relation between the estimated model output *($\hat{y}$)* and the control command sent to the prosthesis *($\hat{y}'$)* can be formulated as,

$$\hat{y}_i' = G_i(\hat{y}_i - T_i) \quad (1)$$

where, $\hat{y}_i$ and $\hat{y}_i'$ are the normalized estimated activations before and after thresholding and gain multiplication, respectively. The subscript i denotes the prosthesis function, specifically, palmar (P), lateral (L), hand open (O), and wrist rotation (R). Finally, the sequential and proportional control was implemented by retaining the maximum value from the set $\{\hat{y}_P, \hat{y}_L, \hat{y}_O, \hat{y}_R\}$ and setting all the remaining values to zero.

2.2.3 Context-aware component (CAC)

In the present prototype, the CAC was implemented as a finite state machine (FSM). The prosthesis operation was modeled through five states, namely, *Free, Preshaped, Grasping, Holding* and *Moving,* representing typical phases arising during grasping and object manipulation. The transition between the states was triggered using online sensor data (Fig. 3). Upon entering a state, a set of rules was activated for post processing of the commands generated by the myoelectric controller (Fig. 4). The rules were designed to improve the robustness of control considering the operational demands and likely disturbances in each of the states. The rules included manipulating the thresholds to decrease/increase the ease of activation of specific functions as well as simple IF-THEN actions (such "restore force" rules).

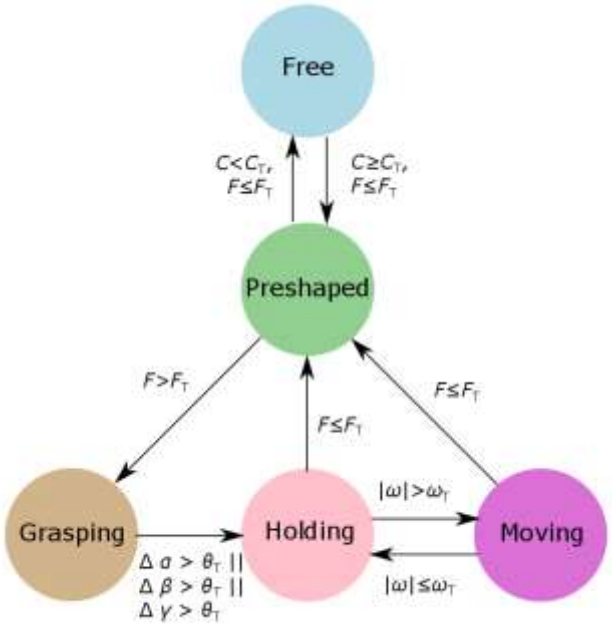

Fig. 3: State machine for context-driven control. The state machine detected five prosthesis states: Free, Preshaped, Grasping, Holding and Moving. The conditions for transition between the states, indicated next to the arrows, were based on comparing the sensor outputs (from embedded inertial, force and aperture sensors) to predefined thresholds. The annotations are: C – normalized grip closure, F – normalized grasping force, (α, β, γ) – elbow orientation and |ω| – elbow angular velocity. The threshold values were: $C_T = 0.2$, $F_T = 0.02$, $\theta_T = 10°$ and $\omega_T = 1$rad/s.

Initially, the hand is open and thereby in the *Free* state (Fig. 3). The thresholds from eq. (1) are set to the default value. Next, the user starts closing the hand (either using palmar or lateral grip) to grasp an object, and the state *Preshaped* is activated to indicate that the hand is configured into a specific grasp, ready to enclose the object. To assist the user in forming a stable grip, the threshold for wrist rotation is increased to reduce the odds of accidental wrist rotation(s) during grip closure. When the force sensor detects contact with the object, the *Grasping* state is activated. In this state, the subject will increase the grasping force, preparing for the object lift off. To stabilize the wrist while the subject modulates the muscle contraction level to adjust the force, the rotation threshold is further increased. The forearm orientation and the achieved grasping force are registered upon entry and exit from this state, respectively.

In the next step, the subject lifts the object. This action is detected by monitoring the difference between the current forearm orientation and the orientation that was registered in the *Grasping* state. In response, the FSM enters the *Holding* state. In this state, the aim is to allow the subject to manipulate

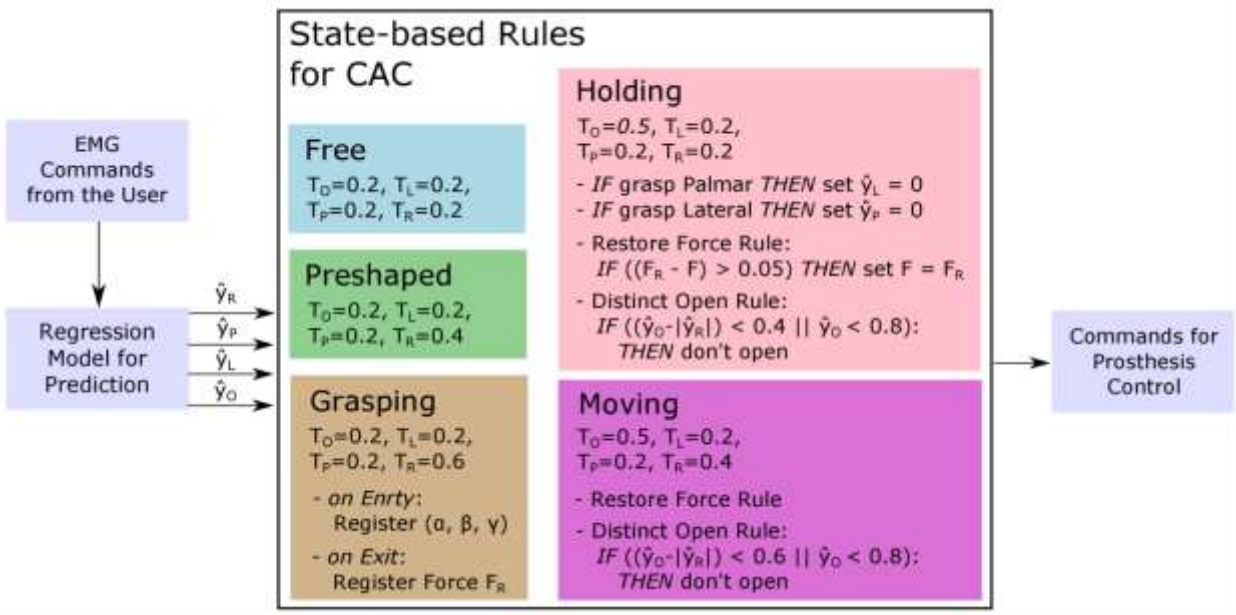

Fig. 4: State based rules for context aware component (CAC). In each of the five prosthesis state, a pre-defined set of rules was used to post-process the outputs of the machine-learning controller. See the text for a detailed description of the rules. The annotations are: R – Rotation, L –Lateral, P – Palmar, O – Hand Opening, T indicates the thresholds for the corresponding signals and $\hat{y}$ indicates the prediction estimate.

the object while preventing the accidental opening of the hand. Therefore, the wrist rotation threshold is decreased back to the default value, and the hand opening threshold is increased. Additionally, to open the hand the subject is required to produce an unambiguous opening command by generating a strong signal without concomitant rotation command. This is enforced by the "*distinct open*" rule, which is active in this state, assuring that the hand opens only when the subject clearly indicates an explicit intention to release the object. This rule does not block all spurious opening commands, but it weakens their effect. A weak spurious opening command can still decrease the applied grasping force, and multiple such commands generated over time can eventually reduce the contact force down to zero, leading to an unintentional dropping of the object. To prevent this, the "*Restore Force"* rule was activated to readjust the grasping force to the level registered when exiting from the *Grasping* state. This was the force level that the subject adjusted as appropriate for the object, just before the object was lifted. The *restore forc*e rule was triggered whenever a force dropped with respect to the registered level. Importantly, the force increase was not affected (i.e., the subject was free to increase the force). Finally, in the *Holding* state, the command for hand closing using the other grasp type was disabled, i.e., if the palmar grip was used to grasp the object, then the lateral grip was disabled and vice versa. Changing the grasp type while the hand is closed (*Holding* state) would cause hand opening and repositioning of the thumb, and thereby unintentional dropping of the object.

Lastly, the *Moving* state was activated when the subject started moving the prosthesis (e.g., to carry the object from place to place). The aim in this state was to stabilize the prosthesis, i.e., to maintain the present grasp and configuration parameters. The assumption was that it is unlikely that the subject would issue the commands to the prosthesis while moving the object. Therefore, the wrist rotation

threshold as well as the threshold for the *distinct open rule* was increased compared to the *Holding* state. Note that none of the prosthesis functions was actually disabled in any of the states; they were just made more or less difficult to activate. Put differently, in some states, the user was required to exert more effort, indicating clear determination to activate a certain function.

3 Experimental Procedure

Ten able-bodied subjects (age 29.4+6.0 years, all male) participated in the experiment, after receiving an oral and written description of the experiment, and signing an informed consent form. The experiment was conducted according to the Declaration of Helsinki and approved by the Ethics Committee at the University Medical Center in Göttingen.

The subjects stood in front of a table with adjustable height, where a box-&-blocks (B&B) test was placed approximately 20 cm away from the subjects. Two types of wooden blocks were used during the experiment (each compliant with a particular prosthesis grip type): *i)* the standard *cubical* wooden block with the side length of 2.5 cm to be grasped using a palmar grip and *ii)* a modified *cuboidal* wooden block with the dimensions of 2.5x3.0x7.5 cm to be grasped using a lateral grip. Before starting the countdown timer, either 30 cubical blocks or 6 cuboidal blocks were placed in the left compartment of the setup. A standard PC monitor was positioned approximately 125 cm away from the subjects to provide visual feedback and task instructions.

The outline of the experimental protocol is shown in Fig. 5(A). After the system *calibration phase*, three different evaluation tasks (arm and wrist positioning, wrist tracking and hand shaking) were successively administered to the subjects. The subjects performed each task using classic control (MYO) and context driven control (cxMYO). In MYO, the outputs of the myoelectric controller were directly used as the commands for prosthesis control, whereas in cxMYO, the outputs were first processed by the context aware component (CAC), as explained in the previous section. In each task, the usage of MYO and cxMYO was randomized across subjects. The experiment was designed specifically to test the robustness of the two control approaches.

In the *calibration phase*, the experimenter explained the concept of myoelectric control and then, the system components were placed on the subject's left arm (as shown in Fig. 2) and the myoelectric controller was trained as explained before. Next, the *arm position detector* was calibrated by asking the subjects to bring their arm in each arm position AP1-4 (Fig. 5(C)), where the *pitch* angle for the forearm and the *pitch* and *yaw* angles for the upper arm were registered. To identify the subjects' arm position during the online test, the measured angles were compared to the registered values and the tolerance threshold was set to 30°. The identification of the arm positions was not used for prosthesis control, but only to ensure that the subject correctly followed the experimental protocol. The subjects were then familiarized with each task by performing it for approximately 5 min using MYO.

After calibration and familiarization, the subjects performed three functional tasks, as outlined in Fig. 5(A). All tasks followed the same structure and had a predefined number of rounds being performed using both control methods (cxMYO and MYO). A *round,* in each task, was defined as a time interval during which the subject performed as many trials as possible. To start a *trial*, the subject picked up a wooden block from the left compartment of the box using the indicated grasp (palmar or lateral). The subject also adjusted the grasping force to be between 30-70% of the maximum prosthesis force, using visual force feedback provided on the computer screen. Once the block was appropriately grasped, the force feedback was removed and the so-called Visual Task Instruction (VTI) was presented on the

computer screen (by the experimenter). The VTI was used to indicate a sequence of actions, which the subject had to perform before returning the block back to the right compartment of the box (end of trial). A trial was deemed *successful* if the block was transferred from the left to the right compartment, whereas if the block was dropped during VTI the trial was considered *failed*. The subjects were allowed to complete the last ongoing trial if it started before the round timer stopped. Lastly, the notion of round and trial was the same in all three functional tasks, i.e., each task comprised several rounds and in each round, the subject did multiple trials. However, the VTI and therefore the requirements in each functional task were different, as described below.

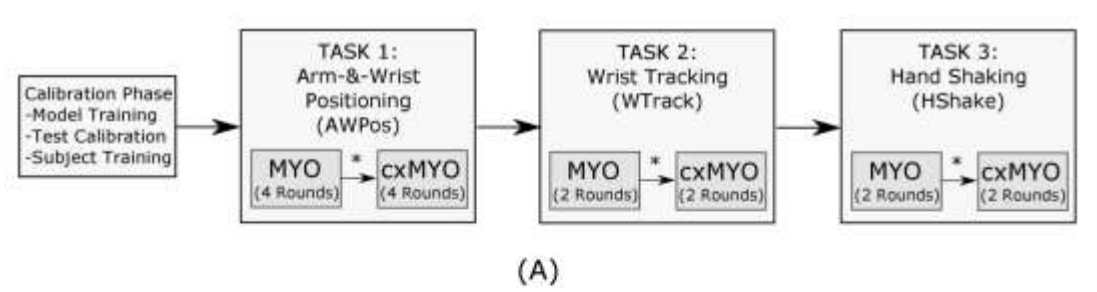

(A)

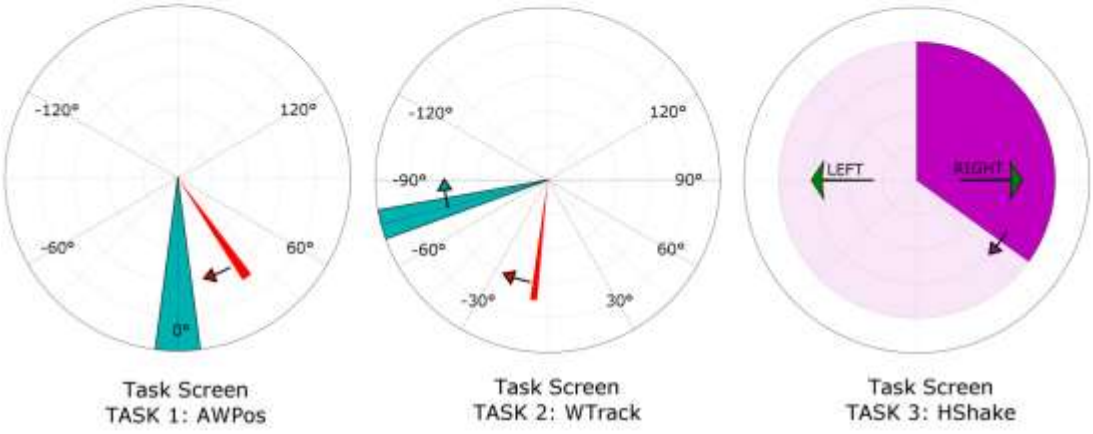

(B)

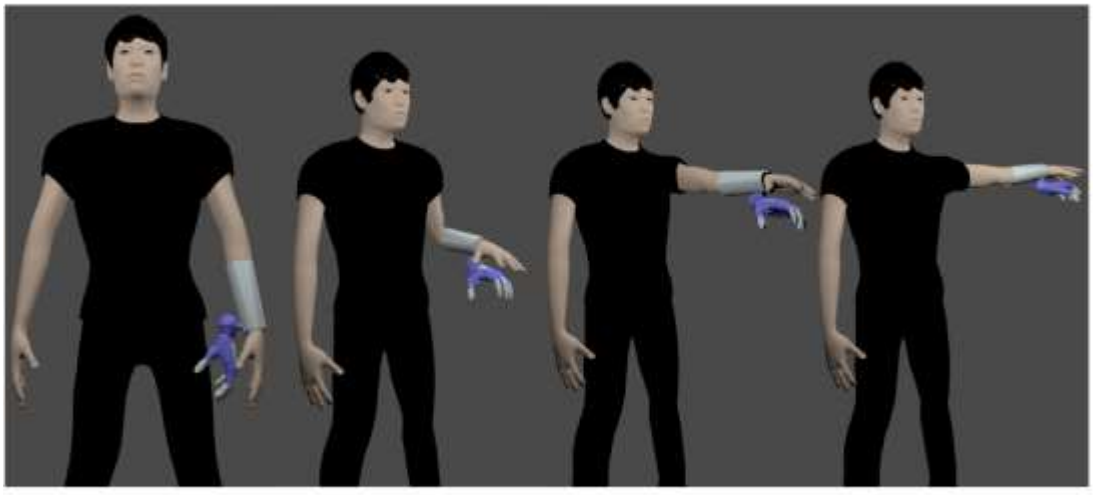

(C)

Fig. 5: (A) Experimental Protocol. Three tasks were administered to the subjects sequentially (AWPos, WTrack and HShake). Each task was performed using classic (MYO) and context-enhanced myoelectric control (cxMYO), where the order of the control methods was randomized (indicated by an asterisk). (B) Visual Task Instruction (VTI) to the subject. In AWPos and WTrack, the dark-cyan pie shape indicated the target wrist position and the red cursor indicated the current position of the prosthetic wrist. The task consisted of rotating the prosthetic wrist from the initial to the target position (AWPos) or to track the moving target (Wtrack). In HShake, the subject shook the forearm in the indicated direction (arrows) until the dark-violet completion-metronome traversed the full circle. (C) Arm Positions. The subjects performed AWPos and WTrack tasks in the four arm positions (AP1 - forearm down, AP2 - elbow flexed, AP3 - arm frontally extended, AP4 - arm laterally extended).

Arm and Wrist Positioning Task (AWPos): The task comprised 4 rounds (two performed using palmar and two using lateral grasp) and each round lasted 4 minutes. In a single trial, the VTI presented four pairs of target-arm and target-wrist positions. First, a random arm position from the set AP1-4 (Fig. 5(C)) was presented as an image on the computer screen. The arm position detector (discussed above) awaited the subject to bring his arm in the required position. Next, the marker (red) and the target area (cyan) indicating the current and desired wrist rotation, respectively, were displayed by the VTI (Fig. 5(B)). The subject was required to move the prosthesis wrist such that the red marker reached the target area (and remained inside it for 250 ms). The target areas were randomly selected from a set of predefined target angles {-120°, -60°, 0°, 60°, 120°} with a tolerance of ±15°. Once the target-wrist position was achieved, a new target-arm position was presented to the subject. This process was repeated four times in a single trial, i.e., each of the four target-arm positions were presented randomly, followed by a random (non-repeating) target-wrist position. Lastly, the arm position detector was used to continuously monitor the subject's arm posture and when a change with respect to the indicated position was detected, the markers indicating the current and the target wrist position (red and cyan marker) were removed from the screen and the VTI requested the subject to reconfigure the arm posture.

Wrist Tracking Task (WTrack): The task comprised 2 rounds (one performed with each of the two grasps) and the round duration was 4 minutes. In a single trial, the VTI presented one target arm position (from the set AP1-4) which remained fixed during the trial. The task for the subject was to keep his arm fixed in the indicated position and control the rotation of the wrist, so that the red marker representing the current wrist position tracked the moving target (desired wrist rotation), as shown in Fig. 5(B). The trajectory for the moving target was generated by randomly selecting eight *center-angles* from the set {-120°, -90°, -60°, -30°, 30°, 60°, 90°, 120°}. The moving target was then rotated between those angles with a velocity randomly selected from the set {30°/s, 45°/s, 60°/s}. The center angles were chosen so that the sign between the consecutive angles would change. In this way, the subjects were challenged to repeatedly pronate and supinate. Additionally, each time the target reached one of the eight center-angles, it stopped until the subject successfully positioned the red marker within the target (center-angle±10°). Thus, a single trial of the WTrack task comprised tracking a moving target on the screen while keeping the arm fixed in a given position.

Hand Shaking Task (HShake): The task included 2 rounds (one with each of the two grasps) and each round lasted 3 minutes. In a single trial, the subject shook the forearm in the direction indicated by the arrows until the completion-metronome traversed the full circle (Fig. 5(B)). The indicated direction of shaking was either *left-and-right* or *up-and-down*. The angular velocity ($|\omega|$) of the elbow joint was measured and used to drive the completion-metronome. The subject was required to generate angular velocities $|\omega|$ between $[\omega_{min}, \omega_{max}]$ for 10 s; and, the completion-metronome indicated the fraction of time for which $|\omega|$ was in the required range. The thresholds $[\omega_{min}, \omega_{max}]$ for left-&-right shake were [2.5, 5] rad/s, whereas for up-&-down shake they were [2, 4.5] rad/s; the difference was due to a greater difficulty of shaking against gravity.

After the experiment, the subjects were required to fill out a questionnaire, evaluating the subjective experience with the two methods. In the questionnaire, the term *Approach 1* and *Approach 2* were used to indicate either MYO or cxMYO – depending upon the sequence in which the randomized modalities were tested. The Questionnaire was divided into three parts as follows: (a) *Physical Demand*: was used to assess the physical demand for each of the three tasks (independent of the control modality). (b) *Control Cognitive Demand*: was used to access the *mental demand* and *frustration level* associated with each control modality, independently of the three tasks. (c) *Control Comparison*: was used to make direct comparison between the two control modalities. (The questionnaire is provided as supplementary material).

3.1 Outcome Measures and Data Analysis

The primary outcome measures from each of the three tasks were the number of *successful* and *failed* trials per round. To compare the performance of MYO and cxMYO more comprehensively, four secondary outcome measures were evaluated offline from the recorded data: a) the number of spurious opening commands, b) the number of spurious closing commands indicating the grasp type opposite to that currently used, c) the mean absolute difference between the normalized grasping force at the beginning and end of the trial, and d) the mean absolute difference between the wrist rotation at the beginning and end of the trial. All the measures were determined for all successful trials in each round, and the last measure was relevant only in the HShake task. For an ideal performance, all secondary metrics should be equal to zero, as the subjects did not attempt to open or close the hand, or change the grip force/grip type during the tasks. In addition, during HShake task, the subjects were not supposed to rotate the hand.

The data were tested for normality and depending on the outcome of the test, a paired t-test or Wilcoxon signed rank test were used to compare the performance of MYO versus cxMYO for the same task. For the questionnaire, the *Task Physical Demand* between the three tasks was compared using the Freidman test followed by a post-hoc average rank test for pairwise comparison. A Wilcoxon signed rank test was used to determine if the secondary measure *Number of Spurious Grasping Commands* was significantly higher than zero (as the count was always zero for cxMYO). All results in the text are reported in terms of median and interquartile range (IQR) – denoted as *median{IQR}*. The software STATISTICA (Dell, US) was used to perform the statistical analysis and the threshold for significance was set to $p < 0.05$.

4 Results

Fig. 6 summarizes the results for the two primary outcome measures obtained by using MYO and cxMYO in the three tasks. When using cxMYO, the subjects performed significantly more successful trials per round in the AWpos (5{4-6} vs. 4{2-5} with $p<0.001$) and HShake (5{5-6} vs. 5{3-6} with $p <0.05$), and they dropped significantly fewer objects per round in all the tasks, 0{0-0} vs. 2{0-3} with $p<0.001$ in AWpos, 0{0-1} vs. 1{0-2} with $p<0.05$ in WTrack, and 0{0-0} vs. 0{0-2} with $p<0.01$ in HShake. In the HShake task, there were no drops when using cxMYO.

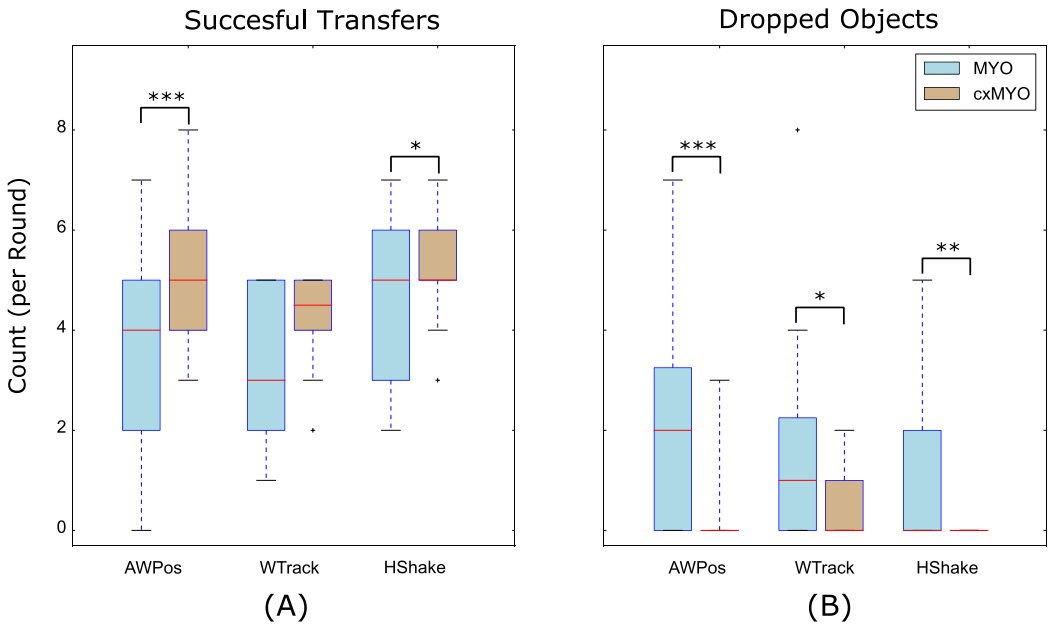

Fig. 6: Summary of the results for primary outcome measures during online tasks with classic (MYO) versus context-driven control (cxMYO): (A) Number of successful object transfers per round. (B) Number of objects dropped (while making a transfer) per round. The box plots indicate medians (red line), interquartile range (boxes), maximum/minimum values (whiskers) and outliers (crosses). Note that context-driven control significantly outperformed the classic control in all but one outcome measure. ('*', p<0.05; '**', p<0.01; '***', p<0.001).

Fig. 7 depicts representative signals recorded during online control illustrating the secondary outcome measures. The prosthesis control was set to MYO in Fig. 7(A, B and D) and cxMYO in Fig. 7(C). In Fig. 7(A), the subject issued four accidental opening commands while performing the AWPos task and this led to an unwanted decrease in the grasping force. This would have been prevented if the cxMYO was used, as all spurious opening commands were below the state-dependent threshold. In Fig. 7(B), the grasping force exerted on the object increased due to spurious grasping commands. The object was grasped using lateral grip, and the subject issued accidental palmar closing command, causing the tightening of the grasp. This would have been prevented with cxMYO, as it disabled closing commands indicating wrong grasp. Fig. 7(C) illustrates that the grasping force gradually decreased with MYO (red line). In some cases, this was a purely mechanical effect, as the object would slip or move in the hand, and sometimes this was produced through "accumulation" of accidental opening commands. With cxMYO, the force was restored whenever a drop in force was detected ("restore force" rule in *Holding* state). In Fig. 7(D), the subject generated unwanted wrist rotation commands toward the end of the trial during the HShake task. All but two of those spurious rotation commands would be blocked by cxMYO, as the spurious signals were below the state-dependent threshold.

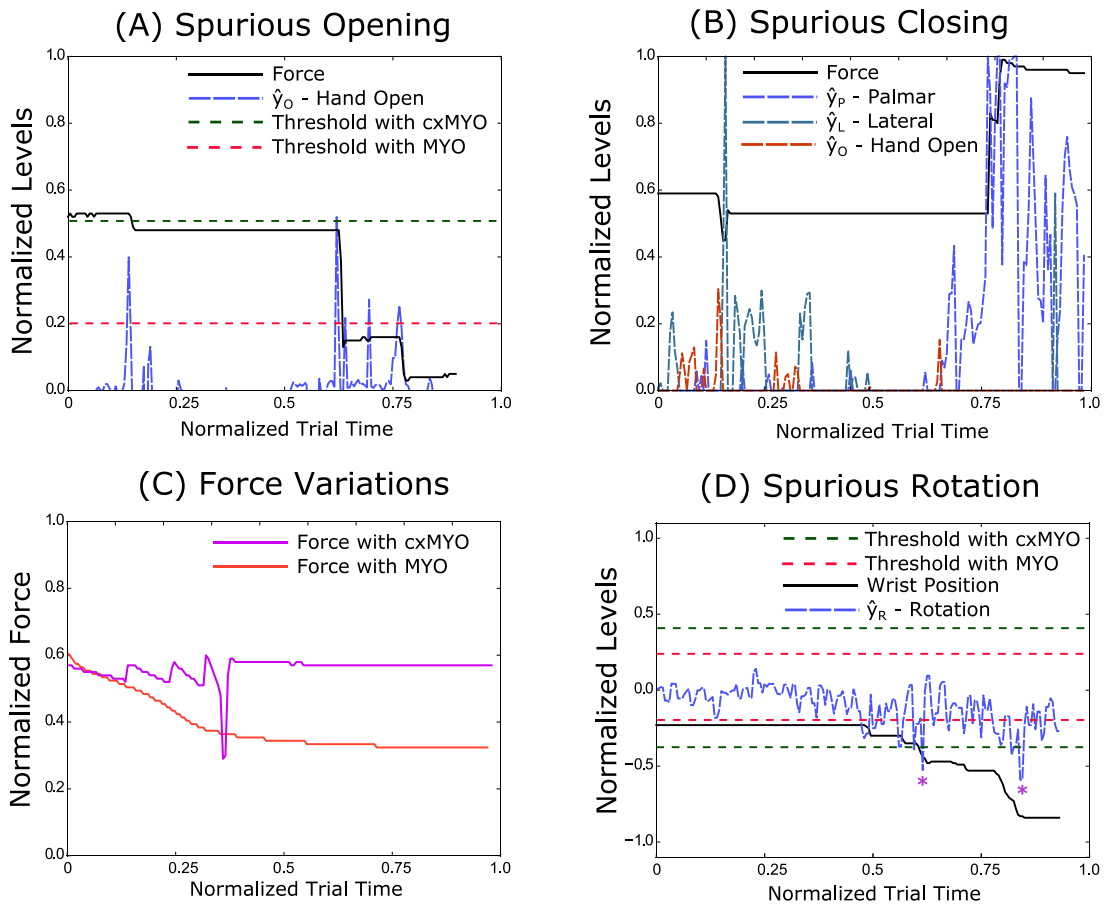

Fig. 7: Representative signals recorded during the experiment, demonstrating the impact of context-driven control (secondary outcome measures): (A) Spurious opening commands (B) Spurious closing commands (C) Force restoration (*Restore Force Rule*). (D) Spurious rotation commands. The prosthesis control was set to classic (MYO) in Figures (A), (B), (C), (D) and context-driven control (cxMYO) in (C). The signals $\hat{y}_P, \hat{y}_L, \hat{y}_O$ and $\hat{y}_R$ are the normalized estimated control signals for palmar closing, lateral closing, opening and rotation, respectively.

The summary results for the secondary outcome measures are depicted in Fig. 8. When cxMYO was active, the number of spurious opening commands was significantly lower compared to MYO for the tasks AWPos (0{0-0.25} vs. 2{0.75-4} with $p<0.001$) and HShake (0{0-0} vs. 1{0-2} with $p<0.01$). Next, there were no spurious closing commands when using cxMYO. During MYO, however, the number of such commands was significantly higher than zero in all three tasks AWPos (1{0-10}, $p<0.001$), WTrack (0.5{0-4.75}, $p<0.01$) and WTrack (1.5{0-3}, $p<0.05$). The absolute change in normalized grasping force for the trials with cxMYO was significantly lower than MYO for the task AWPos (0.05{0.03-0.075} vs. 0.1{0.0375-0.175} with $p<0.01$) and HShake (0.04{0.02-0.05} vs. 0.085{0.03-0.13} with $p<0.05$), whereas the variation in force was similar for task WTrack (0.06{0.04-0.1} vs. 0.047{0.02-0.10} with $p>0.05$). Finally, for the HShake task, the unwanted wrist rotation in trials with cxMYO was significantly lower than MYO (15°{4°-32°} vs. 40°{7°-85°} with $p<0.05$).

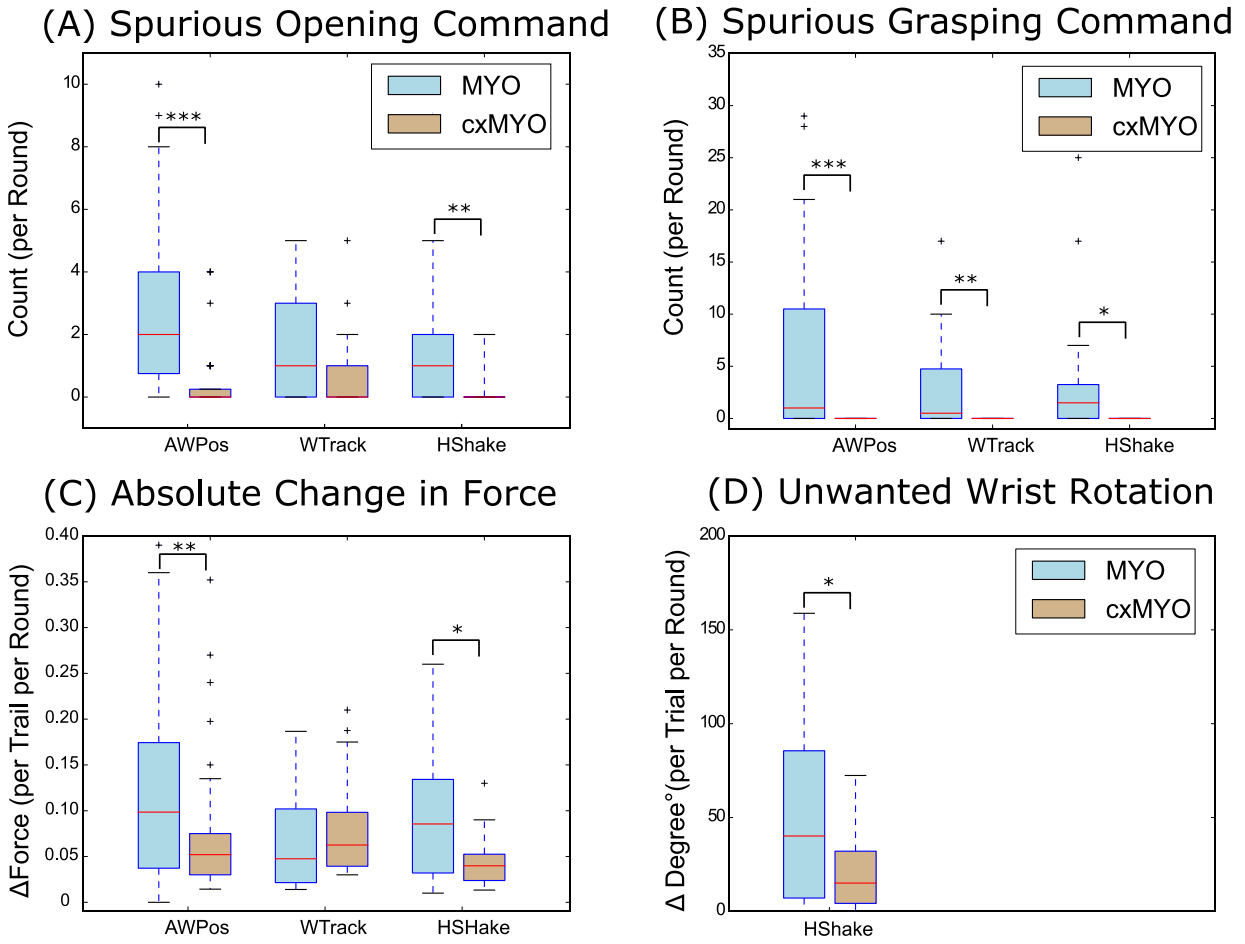

Fig. 8: Summary of the results for secondary outcome measures during online tasks with classic (MYO) versus context-driven control (cxMYO): (A) Number of spurious opening commands generated during successful trials in each round. (B) Number of spurious palmar/lateral closing commands generated during successful trials in each round. (C) Change in normalized grasping force from start till the end of successful trials in a given round. (D) Change in wrist position from start till the end of successful trials in a given round (HShake task only). The box plots indicate medians (red line), interquartile range (boxes), maximum/minimum values (whiskers) and outliers (crosses). (*'*', p<0.05; '**', p<0.01; '***', p<0.001*)

The summary results for the questionnaire are shown in Fig. 9. The physical demand for the task WTrack was significantly higher than for the tasks AWPos and HShake (70{60-78.75} vs. 40{35-65} and 70{60-78.75} vs. 55{35-55}, with *p<0.05*). We think that the constraint of fixing the arm in one position (especially AP3 and AP4) during some trials led the subjects to experience a higher physical demand for the WTrack task. The reported frustration with MYO was significantly higher than with cxMYO (75.5{41-65} vs. 37.5{31-52.5} with *p<0.05*) whereas the mental demand required for both control approaches was similar (55{31.5-70} vs. 37.5{26.5-52.5} with *p>0.05*). Fig. 9(C) characterizes direct, point by point comparison between MYO and cxMYO. With cxMYO, the subjects reported being more confident about not dropping the grasped object, with the median response 40{0-50} significantly higher (*p<0.05*) than zero. The rating was not significantly different from zero for any of the other measures.

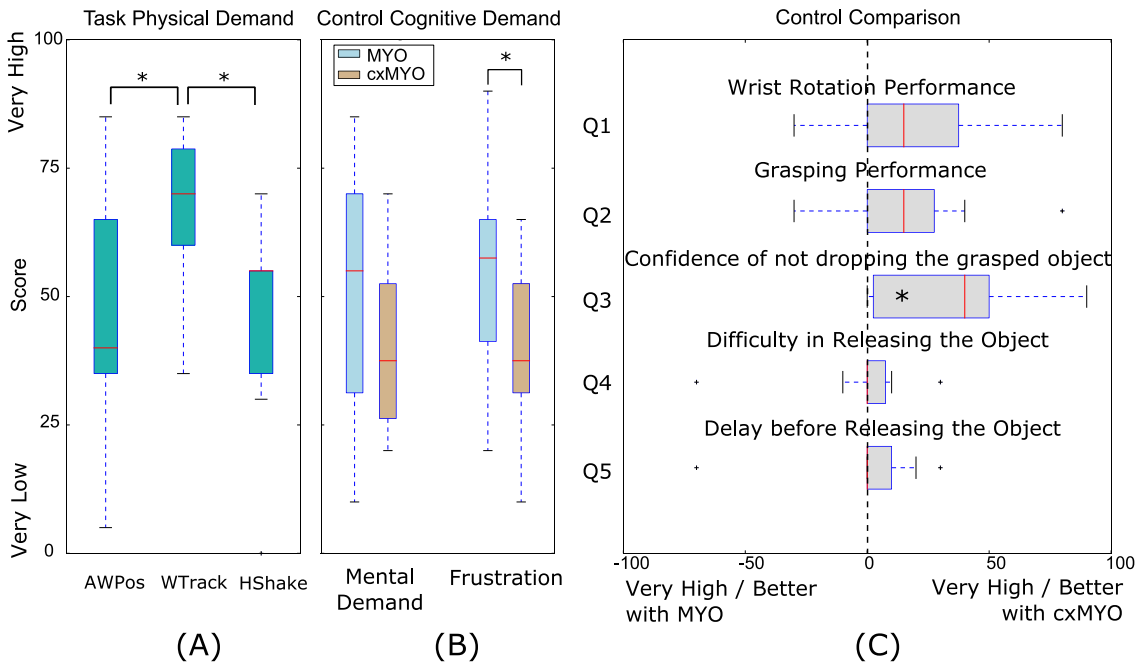

Fig. 9: Summary of the results for the questionnaire. (A) Physical demand across tasks. (B) Cognitive demand across control methods. (C) Control performance comparison. Subjects indicated significantly less frustration and more confidence when using context-driven control. (*'*', p<0.05; '**', p<0.01; '***', p<0.001*).

5 Discussion

A new concept of context-driven control (cxMYO) for upper-limb prostheses has been introduced and extensively compared with classic myocontrol (MYO) using three functional tasks specifically designed to challenge the robustness of prosthesis control. The results demonstrated that the cxMYO significantly improved the performance in each of the three tasks. In cxMYO, the information from the prosthesis sensors was used to estimate the prosthesis state (context) and then increase the robustness of the myoelectric controller to expected disturbances by applying a set of simple post processing rules. The cxMYO substantially suppressed the spurious opening, closing and rotation commands, as well as stabilized the grasping force. This resulted in an improved task performance, better success and lower drop rates, and increased subject satisfaction.

The aim of the present study was to assess the robustness of the novel versus conventional approach (cxMYO vs. MYO). Therefore, we have carefully designed a set of functional tasks to substantially challenge the robustness of myoelectric control. The tasks integrated several factors that are known to cause problems in the operation of a myoelectric prosthesis, such as: 1) changing the position of the arm (AWPos), 2) performing rapid arm movements (HShake), and 3) generation of myoelectric commands in rapid succession (WTrack). As the prosthesis was mounted on the subject, the effect of added weight was also considered in the tests. It is known that repositioning the arm changes the muscle patterns and therefore leads to misclassifications. This problem is addressed in several recent studies [15], [16], [25], [26]. Similarly, fast arm movements, such as shaking, can generate spurious muscle activations and thereby unintentional prosthesis responses (e.g., hand opening/closing and object dropping/breaking). In the past, the shaking test was used to demonstrate the robustness of osseointegration [27] against motion artifacts observed during real-life use, as shown in the movie [28].

Finally, rapid generation of commands is characterized with many transient muscle activations, which could lead to possible misclassifications [29], [30]. Although using clinical tests (e.g., SHAP [31]) would be useful for cross study comparability, none of the standard tests include these challenging factors to a sufficient extent. Therefore, we decided to use custom-made tasks. Nevertheless, we do intend to perform a clinical assessment in the future, when we improve the experimental setup so that the system components can be integrated into the prosthetic socket. This is an important step as practical mounting and good interface between the subject and the system can have substantial impact on the clinical results.

Context information has been used to implement automatic prosthesis control in the past [12], [13], [19], [20], [21], [22] and only recently to improve the performance of a machine learning controller [15], [16]. The present study advances the state of the art in the latter direction by presenting a method to utilize multimodal sensing to improve the robustness of an advanced machine learning controller. We propose a different paradigm compared to [15], [16]. The context information in [15] and [16] was derived only from inertial sensors and along with EMG, it was given as an "input" to the classification-framework, hence the conventional black box approach. In the novel method, the context was modeled explicitly as a state machine describing the prosthesis operation and the data was handled by a dedicated component (CAC in Fig. 1) detecting the states online. The CAC, then, modulated the outputs of the MYO controller. This allows more flexibility and generality, as each state modulates the MYO to increase robustness against expected disturbances specific to that state. In [15] and [16], the context information was used to mitigate the impact of a single factor (arm position). In cxMYO, however, *Preshaped* and *Grasping* states stabilized the hand against unwanted rotations, *Holding* prevented accidental opening and force decrease, and *Moving* filtered out spurious rotations and openings. Finally, the models proposed in [15] and [16] were evaluated offline using EMG data collected in static conditions and they did not consider the interaction of the user with the control system in real-life situations. The cxMYO is substantially different from the methods for context-based automatic control [12], [13], [19], [20], [21], [22], as the context processing operates in the background and does not directly influence the online control. Hence, the online control in cxMYO always remains *manual,* i.e., each prosthesis function is activated only in response to command(s) generated by the subject. The subject could activate any command in any moment and the CAC merely modulated the manual control (MYO), so that some commands in certain states required a stronger and/or clearer muscle activation. As demonstrated in the present experiment, this has significantly improved the robustness of manual control based on machine learning.

In the present study, the context information was used to influence only the post-processing parameters of the machine learning algorithm (mostly, activation thresholds). Nevertheless, the concept is general and can be used to influence other extrinsic as well as intrinsic parameters of any myoelectric controller. For example, the gains can be modulated depending on the prosthesis state. This could be used to provide more sensitive force control during object holding or manipulation. In the prosthesis used for this study (Michelangelo hand), it is difficult to decrease the force without opening the hand when holding a rigid object. To address this issue, the prosthesis can be made less responsive by lowering the gain of the hand opening while in *Holding* state. Furthermore, the likelihood of activating specific prosthesis functions can change depending on the state of the prosthesis. For example, it is unlikely to start rotating the hand while closing it around an object. Therefore, the state information could be used to modify the prior probability of occurrence associated to each function. This is equivalent to an online update of the classification boundaries between the classes in a myoelectric classifier and can potentially further reduce the spurious opening, grasping and rotation commands and thereby increase the user's confidence in the system. The present method was based on simple post

processing and therefore it is convenient for real-time implementation. The states were detected and post processing was implemented using simple IF-THEN rules operating on thresholds. Interestingly, a common set of threshold values could be used across all subjects with good performance, which additionally demonstrates the robustness of the approach. In the future, more advanced methods (e.g., hidden Markov models [32]) could be used for state detection and parameter modulation.

The present experiment demonstrated that the use of context-aware component increased robustness of myoelectric control. However, the experimental evaluation was performed in naive able-bodied subjects, a test population which is different compared to skilled (or naive) amputee users. In this study, all able-bodied subjects consistently used flexion, extension, closed-fist, ulnar and radial deviation to control the five prosthesis functions, whereas amputees might use different activation patterns depending on the anatomy of the remaining forearm muscles. Therefore, the quality of myoelectric control in terms of reliability and robustness is likely to be different. For example, in case of a short residual limb with less musculature to provide signals, the patterns might be less discriminable, leading to more misclassifications (poorer performance of MYO). This could further emphasize the utility of cxMYO compared to MYO alone, as the CAC aims at improving the robustness of MYO. Also, depending upon experience, amputees can use grasping/manipulation strategies which are substantially different from able-bodied subjects. With the use of prosthesis, the subjects are expected to improve the consistency and discriminability of their muscle activation patterns. In an experienced user, the MYO performance can be already so good that the contribution of CAC becomes redundant. Therefore, CAC could be implemented as an optimal component, i.e., initially activated to support a naive user and then deactivated once the user becomes experienced. In the future, we will improve the setup so that it can be integrated into a prosthetic socket to test the system in a pool of male and female amputee subjects.

Improving the robustness of myoelectric control is an important challenge towards facilitating a wider clinical application of these methods for prosthesis control. To this aim, invasive techniques such as osseointegration [27] and implanted systems for EMG recording [33] are investigated with promising results. Non-invasively, the performance can be improved using alternative and multimodal sensing (e.g., sonography [3]) but this research is still in the initial phase. The present study demonstrates that myoelectric control can be substantially improved also by exploiting sensors that are already available in the prosthesis or that can be easily integrated into it. This is a simple, non-invasive and cost-effective approach to improve the stability in myoelectric control with surface EMG electrodes.

Acknowledgments

We acknowledge financial support by the German Ministry for Education and Research (BMBF) under the project INOPRO (16SV7657). The authors would like to thank Mr. Hemant Karna of UMG for his support in developing the test protocol. The graphs and figures presented in the manuscript were created using Inkscape (www.inkscape.org) and Matplotlib with Python 3.3 on the Anaconda framework (www.matplotlib.org, www.python.org and www.continuum.io).

Appendix

Incremental Ridge Regression with Random Fourier Features (iRR-RFF): In machine learning, problems related to linearity of the system can be circumvented by using a basis function [34], [35]; which involves preprocessing each sample with a non-linear mapping function $\Phi: \mathbb{R}^d \longrightarrow \mathbb{R}^{\mathcal{D}}$. The choice of Φ is obviously crucial and in the case of iRR-RFF [23], Φ involves the application of sinusoidal functions to the samples; which per se includes a finite-dimensional approximation of a Gaussian kernel [36].

$$\Phi(x) = \cos(\omega_{\mathcal{D}\times d} * x_{d\times 1} + b_{\mathcal{D}\times 1})$$

Here, d (=8) is the number of surface EMG channels and the non-linear transformation Φ projects the vector $x_{d\times 1}$ to a higher-dimensional feature-space with $\mathcal{D}$ dimensions. The basis function is initialized by drawing $\omega_{\mathcal{D}\times d}$ values from a normal distribution and $b_{\mathcal{D}\times 1}$ values from a uniform distribution. The transformed data $\Phi(x)$ can, then, be used for both learning and prediction according to equations of Ridge Regression, as described in [23]. Theoretically speaking, the RFF basis function is a finite dimensional approximation of the popular Radial Basis Function (RBF) [36]. But, the advantage of using RFF is that it has a bounded computational requirement, supports incremental learning and in practice provides a good approximation for the RBF kernel, when the transform size $\mathcal{D}$ is set to 300 (as demonstrated experimentally in [23]).

References

[1] N. Jiang, S. Dosen, K.-R. Müller, and D. Farina, "Myoelectric control of artificial limbs: is there the need for a change of focus?," *IEEE Signal Process. Mag.*, vol. 29, no. 5, pp. 149–152, 2012.

[2] E. Biddiss and T. Chau, "Upper-limb prosthetics: critical factors in device abandonment," *Am J Phys Med Rehabil*, vol. 86, no. 12, pp. 977–987, 2007.

[3] Y. Fang, N. Hettiarachchi, D. Zhou, and H. Liu, "Multi-modal sensing techniques for interfacing hand prostheses: A review," *IEEE Sens. J.*, 2015.

[4] C. Castellini *et al.*, "Proceedings of the first workshop on Peripheral Machine Interfaces: Going beyond traditional surface electromyography," *Front. Neurorobot.*, vol. 8, no. 22, p. 22, Aug. 2014.

[5] M. Asghari Oskoei and H. Hu, "Myoelectric control systems—A survey," *Biomed. Signal Process. Control*, vol. 2, no. 4, pp. 275–294, Oct. 2007.

[6] A. Fougner, O. Stavdahl, P. J. Kyberd, Y. G. Losier, and P. A. Parker, "Control of Upper Limb Prostheses: Terminology and Proportional Myoelectric Control—A Review," *IEEE Trans. Neural Syst. Rehabil. Eng.*, vol. 20, no. 5, pp. 663–677, Sep. 2012.

[7] Guanglin Li, A. E. Schultz, and T. A. Kuiken, "Quantifying Pattern Recognition—Based Myoelectric Control of Multifunctional Transradial Prostheses," *IEEE Trans. Neural Syst. Rehabil. Eng.*, vol. 18, no. 2, pp. 185–192, Apr. 2010.

[8] P. A. Parker, K. Englehart, and B. Hudgins, "Myoelectric signal processing for control of powered limb prostheses," *J. Electromyogr. Kinesiol.*, vol. 16, no. 6, 2006.

[9] "Coapt // Home Page." .

[10] J.-Y. Guo, Y.-P. Zheng, H.-B. Xie, and T. K. Koo, "Towards the application of one-dimensional sonomyography for powered upper-limb prosthetic control using machine learning models,"

Prosthet. Orthot. Int., vol. 37, no. 1, pp. 43–49, Feb. 2013.

[11] A. Radmand, E. Scheme, and K. Englehart, "High-density force myography: A possible alternative for upper-limb prosthetic control," *J. Rehabil. Res. Dev.*, vol. 53, no. 4, pp. 443–456, 2016.

[12] D. Novak and R. Riener, "A survey of sensor fusion methods in wearable robotics," in *Robotics and Autonomous Systems*, 2015.

[13] J. Gonzalez-Vargas *et al.*, "Human-Machine Interface for the Control of Multi-Function Systems Based on Electrocutaneous Menu: Application to Multi-Grasp Prosthetic Hands," *PLoS One*, vol. 10, no. 6, p. e0127528, Jun. 2015.

[14] K. Dermitzakis, A. H. Arieta, and R. Pfeifer, "Gesture recognition in upper-limb prosthetics: a viability study using dynamic time warping and gyroscopes.," *Conf. Proc. IEEE Eng. Med. Biol. Soc.*, vol. 2011, pp. 4530–3, Jan. 2011.

[15] A. Fougner, E. Scheme, A. D. C. Chan, K. Englehart, and Ø. Stavdahl, "Resolving the Limb Position Effect in Myoelectric Pattern Recognition," *IEEE Trans. Neural Syst. Rehabil. Eng.*, vol. 19, no. 6, pp. 644–651, Dec. 2011.

[16] Y. Geng *et al.*, "Toward attenuating the impact of arm positions on electromyography pattern-recognition based motion classification in transradial amputees," *J. Neuroeng. Rehabil.*, vol. 9, no. 1, p. 74, 2012.

[17] M. Markovic, S. Dosen, C. Cipriani, D. B. Popović, and D. Farina, "Stereovision and augmented reality artificial proprioception for closed loop control of grasping," *J. Neural Eng.*, vol. 14, 2014.

[18] M. Marković, S. Dosen, D. B. Popović, B. Graimann, and D. Farina, "Computer vision and sensor fusion for semi-autonomous control of a multi degree-of-freedom prosthesis," *J. Neural Eng.*, vol. submitted, 2015.

[19] D. P. J. Cotton, P. H. Chappell, A. Cranny, N. M. White, and S. P. Beeby, "A Novel Thick-Film Piezoelectric Slip Sensor for a Prosthetic Hand," *IEEE Sens. J.*, vol. 7, no. 5, pp. 752–761, May 2007.

[20] R. Tomovic and G. Boni, "An adaptive artificial hand," *IRE Trans. Autom. Control*, vol. 7, no. 3, pp. 3–10, Apr. 1962.

[21] P. J. Kyberd and P. H. Chappell, "The Southampton Hand: an intelligent myoelectric prosthesis.," *J. Rehabil. Res. Dev.*, vol. 31, no. 4, pp. 326–34, Nov. 1994.

[22] C. M. Light, P. H. Chappell, B. Hudgins, and K. Engelhart, "Intelligent multifunction myoelectric control of hand prostheses.," *J. Med. Eng. Technol.*, vol. 26, no. 4, pp. 139–46, Jan. 2002.

[23] A. Gijsberts *et al.*, "Stable myoelectric control of a hand prosthesis using non-linear incremental learning," *Front. Neurorobot.*, vol. 8, no. 8, 2014.

[24] J. M. Hahne *et al.*, "Linear and Nonlinear Regression Techniques for Simultaneous and Proportional Myoelectric Control," *IEEE Trans. Neural Syst. Rehabil. Eng.*, vol. 22, no. 2, pp. 269–279, 2014.

[25] A. Radmand, E. Scheme, and K. Englehart, "High-density force myography: A possible alternative for upper-limb prosthetic control," *J. Rehabil. Res. Dev.*, vol. 53, no. 4, pp. 443–456, 2016.

[26] Z. G. Xiao and C. Menon, "Performance of Forearm FMG and sEMG for Estimating Elbow, Forearm and Wrist Positions," *J. Bionic Eng.*, vol. 14, no. 2, pp. 284–295, 2017.

[27] M. Ortiz-Catalan, B. H akansson, R. Br anemark, B. Håkansson, and R. Brånemark, "An osseointegrated human-machine gateway for long-term sensory feedback and motor control of artificial limbs," *Sci. Transl. Med.*, vol. 6, no. 257, p. 257re6–257re6, 2014.

[28] "Mind-controlled neuroprosthetics - YouTube." [Online]. Available: https://www.youtube.com/watch?v=ZuJu_uIpvq4.

[29] M. Ison and P. Artemiadis, "The role of muscle synergies in myoelectric control: trends and challenges forsimultaneous multifunction control," *J. Neural Eng.*, vol. 11, 2014.

[30] T. Lorrain, N. Jiang, and D. Farina, "Influence of the training set on the accuracy of surface EMG

classification in dynamic contractions for the control of multifunction prostheses," *J. Neuroeng. Rehabil.*, vol. 8, no. 25, pp. 1–9, 2011.

[31] C. M. Light, P. H. Chappell, and P. J. Kyberd, "Establishing a standardized clinical assessment tool of pathologic and prosthetic hand function: Normative data, reliability, and validity," vol. 83, no. 6, Jun. 2002.

[32] A. D. C. Chan and K. B. Englehart, "Continuous Myoelectric Control for Powered Prostheses Using Hidden Markov Models," *IEEE Trans. Biomed. Eng.*, vol. 52, no. 1, pp. 121–124, Jan. 2005.

[33] P. F. Pasquina *et al.*, "First-in-man demonstration of a fully implanted myoelectric sensors system to control an advanced electromechanical prosthetic hand.," *J. Neurosci. Methods*, pp. 1–9, Aug. 2014.

[34] C. Saunders, A. Gammerman, V. Vovk, and R. Holloway, "Ridge Regression Learning Algorithm in Dual Variables," *Proc. Fifteenth Int. Conf. Mach. Learn. (San Fr. CA)*, 1998.

[35] R. Rifkin, G. Yeo, and T. Poggio, "Regularized Least-Squares Classification," *Adv. Learn. Theory Methods, Model Appl.*, vol. 190 of NAT, no. Science Series III: Computer and Systems Sciences Chapter 7, 2003.

[36] A. Rahimi and B. Recht, "Uniform Approximation of Functions with Random Bases," in *Allerton Conference on Communication Control and Computing (Allerton08)*, 2008, pp. 555–561.